

Traversable Wormholes with Spontaneous Symmetry Breaking

Soumya Chakrabarti^{*1} and Chiranjeeb Singha^{†2}

¹ School of Advanced Science, Vellore Institute of Technology Vellore, Tiruvalam Rd, Katpadi, Tamil Nadu 632014 India

²Inter-University Centre for Astronomy and Astrophysics, Pune 411007, India

November 21, 2024

Abstract

We present an exact, spherically symmetric, static solution of the Einstein field equations minimally coupled to a self-interacting scalar field. The solution does not exhibit any zero proper volume singularity at the center, and therefore, curvature scalars are always regular. We study the property of radial null geodesics and derive that the metric can describe either a two-way or a one-way traversable wormhole depending on certain parameter ranges. Notably, it lacks a Schwarzschild limit. The scalar field exhibits spontaneous symmetry breaking within the coordinate range where a wormhole throat forms. It can be seen as a suggestion that spontaneous symmetry breaking may act as a threshold for wormhole throat formation. Additionally, we compute the radius of the photon sphere, the Lyapunov exponent, the shadow radius, and the innermost stable circular orbits for this spacetime metric.

1 Introduction

Although the General Theory of Relativity (GR) is widely regarded as the most accurate description of gravity to date, the number of exact solutions to its field equations remains relatively small. This limitation is primarily due to the fundamental challenges involved in solving the coupled partial differential equations that form the basis of the theory. In any case, the spherically symmetric field equations of GR are inherently quite restrictive. A clear example of this rigidity is found in the fact that, for a vacuum (where $T_{\mu\nu} = 0$), the Schwarzschild solution stands as the unique static and isotropic solution that satisfies the condition of asymptotic flatness [1–3]. This result is central to the formulation of Jebsen-Birkhoff’s theorem [4, 5]. The Schwarzschild solution represents a singularity with zero proper volume, surrounded by a horizon, and depends on two parameters: r_s , which indicates the location of the horizon, and r , which defines the position of the singularity. When matter is incorporated into the field equations, they become even more restrictive and less predictable. Some partial solutions have been obtained in specific cases, such as GR coupled to self-interacting scalar fields of dilaton or axion types or when coupled to Maxwell electrodynamics or a Yang-Mills field. However, static field configurations in GR are heavily constrained outside the event horizon, as demonstrated by the no-hair theorems.

*soumya.chakrabarti@vit.ac.in

†chiranjeeb.singha@iucaa.in

For a simple minimally coupled self-interacting scalar field ϕ , the contribution to the energy-momentum tensor is written as

$$T_{\mu\nu}^{\phi} = \partial_{\mu}\phi\partial_{\nu}\phi - g_{\mu\nu} \left[\frac{1}{2}g^{\alpha\beta}\partial_{\alpha}\phi\partial_{\beta}\phi - V(\phi) \right]. \quad (1)$$

$V(\phi)$ is the self-interaction of the scalar field. The scalar field profile is imposed upon by a requirement that an $r \rightarrow \infty$ limit should generate a constant value of the scalar field $\phi(r)$ (one can choose to normalize this constant value to zero). Alongwith this, a requirement of asymptotic flatness dictates that the self-interaction potential should have a local extremum at the origin of the scalar field. In fact, we can use these conditions to demonstrate the *no-hair* theorem starting from the scalar field evolution equation

$$\partial_{\mu}\sqrt{-g}g^{\mu\nu}\partial_{\nu}\phi = \sqrt{-g}\frac{dV}{d\phi}. \quad (2)$$

For a static case, only the g^{rr} term contributes to the above equation. We multiply the equation with $\phi(r)$ and do integration by parts from the horizon to infinity, yielding:

$$[\phi g^{rr}\sqrt{-g}\partial_r\phi]_h^{\infty} - \int_h^{\infty} dr\sqrt{-g}g^{rr}(\partial_r\phi)^2 = \int_h^{\infty} dr\sqrt{-g}\phi\frac{dV}{d\phi}. \quad (3)$$

Usually, one realizes a horizon h at the largest zero of g^{rr} . Thus in principle it is possible to integrate the above equation for all $g^{rr} \geq 0$. If we assume regularity of ϕ and $\sqrt{-g}$ at the horizon, then the boundary terms can be dropped (also keeping in mind an asymptotic fall-off of $\phi(r)$ as $r \rightarrow \infty$). In this context, the condition $\phi\frac{dV}{d\phi} \geq 0$ for all $r \geq h$ essentially implies that the self-interaction potential has a local minimum at $\phi = 0$ and no local maximum in the ϕ -range considered outside the horizon. Under this condition, the integrands on both sides of the above equation are clearly non-negative. However, the integral on LHS brings in a negative sign, and for consistency, one must require that both sides of the equation should vanish identically. Thus, the scalar field remains at $\phi(r) = \phi_0 = 0$, its asymptotic value and the resulting metric solution simply generates a Schwarzschild metric. This effectively rules out non-trivial scalar deformations of the Schwarzschild metric within a limit. The scalar *no-hair* theorem demonstrated is now a popular avenue of research [6–10]; however, there remains a curiosity if one can solve a system of static scalar field embedded within GR and weaken this constraint, even if slightly.

There are two further arguments which can provide strong impetus behind the *curious case of a scalar field* coupled to GR. The first argument is a motivation related to the study of cosmic expansion. In a spatially homogeneous cosmological universe, there is an omnipresent requirement of an entity beyond standard matter capable of accommodating the idea of an accelerated expansion [11–15]. A scalar field with a suitably chosen interaction profile has served as the most popular candidate in this pursuit [16, 17]. The present scope of simple scalar field cosmological models appears to be quite bleak in light of the steep fifth force constraints on the baryon-quintessence interaction profile [18]; nevertheless, scalar fields remain capable of generating solutions of considerable interest. As a specific example, one can cite the pseudo-Nambu-Goldstone-Boson (pNGB) model [19] as well as the models where a scalar field is capable of manipulating self-interaction via screening mechanisms [20–22].

The second argument is the requirement of a (grand) unified theory of natural interaction, which should exhibit two crucial components: an underlying Lagrangian formalism to generate the equations of motion and the necessary fundamental couplings. In practice, these couplings do not have any direct derivations, and therefore, they are treated as constant parameters somehow related to the characteristic

scale of interaction. The idea of variation of these couplings was proposed by Dirac as the ‘*Large Numbers hypothesis*’ [23]. There have been quite a few attempts to successfully accommodate this hypothesis within a theory of gravity using interacting scalar fields; however, all of them are partially complete. One of the well-established attempts is the field-theoretic description allowing variations in the Newtonian gravitational constant, the Brans-Dicke (BD) theory [24–26]. In a BD theory, the scalar field is geometric (mass dimension two in natural units) and can be considered with or without any additional interaction. On the other hand, there are propositions of the theory of gravity accommodating the variation of $\alpha = \frac{e^2}{\hbar c}$, the fine structure constant. In such a theory, a scalar field interacts with the charged matter distribution of the universe and drives the variation of an e -field [27, 28]. Theories of this kind are usually associated with atleast a local violation of the equivalence principle, for example, a variation in electric charge e leads to a breakdown of local charge conservation [28]. There are quite a few attempts found in the literature to reproduce such variations within GR [29, 30] and overall, it is difficult to rule out the possibility of a common background mechanism that controls all such variation, although this has never been proved theoretically or experimentally. Intuitively, it can be a way forward to explore the features of a scalar field that can describe a variation in any of the fundamental couplings. Such a scalar field can not be termed *exotic* as it has some motivations from fundamental interactions other than gravity. In this article, we work with a lagrangian where a minimally coupled self-interacting scalar field is capable of inducing spontaneous symmetry breaking. The self-interaction of the scalar field can be compared to a Higgs-like field with a small adjustment in the quadratic term,

$$V(\phi) = V_0 + M(\phi)\phi^2 + \lambda\phi^4. \quad (4)$$

While one can consider λ as a dimension-less parameter of the theory, $M(\phi)$ can lead to an evolving Higgs VEV ν , calculated as

$$\left. \frac{\partial V}{\partial \phi} \right|_{\nu} = 0 \quad , \quad \nu = \sqrt{\frac{-2M(r)}{\lambda}}. \quad (5)$$

It is to be noted that ϕ need not necessarily be the standard model Higgs. We can imagine the standard model Higgs φ having two components, the Higgs particle h alongwith a classical background field ϕ , with a corresponding Lagrangian given by

$$L = -\frac{1}{2}\partial_{\mu}\varphi\partial^{\mu}\varphi - \frac{\lambda}{4}(\varphi^2 - \nu^2)^2 \quad , \quad \varphi = \nu_0 + \phi + h = \nu(\phi) + h. \quad (6)$$

Due to this construction, the Higgs VEV ν can exhibit an evolution as a function of the classical field ϕ . This variation plays an important role in the electroweak theory of interactions, where the Higgs boson is thought to be the mass generator of quarks. There is a linear correlation between the quark mass and Higgs VEV, $m_{e,q} = \lambda_{e,q}\nu$, where $\lambda_{e,q}$ is the Yukawa coupling [31–34]. While the quark masses are directly proportional, the VEV contribution to proton mass m_p can be neglected since it depends primarily on the scale of quark-gluon interaction. As a consequence, any pre-assigned variation in VEV results in a variation of the proton-to-electron mass ratio μ , which is directly measurable through the observation of molecular absorption spectra [35–38].

In this manuscript, we present a new exact spherically symmetric static solution of the Einstein field equation coupled with a self-interacting scalar field. The self-interaction of the scalar field is in the form written in Eq. Eq. (4). The static solution has no zero proper volume singularity at $r = 0$. The curvature scalars are also non-singular for all coordinate ranges. We study the behavior of radial null geodesics

for this solution and explain that depending on the regions of parameter space under consideration, the solution can describe a two-way or a one-way traversable Wormhole. The requirement for non-trivial static solutions of the field equations of GR as well as of extensions of GR has always been steadfast. Usually these solutions describe wormholes and/or (regular) black holes (see for instance, [39–52] for recent literature). The solution we discuss is unique primarily because it has no Schwarzschild limit. Moreover, the scalar field behaves as a constant in the asymptotic limit and exhibits spontaneous symmetry breaking within the coordinate range associated with the formation of a wormhole throat. In other words, we demonstrate that spontaneous symmetry breaking can be viewed as a threshold for the formation of a wormhole throat. Furthermore, we calculate the radius of the photon sphere, Lyapunov exponent, shadow radius, and innermost stable circular orbits for this spacetime and discuss their nature.

2 An Exact Solution and its Properties

The gravitational action we consider has the following form

$$S = \int d^4x \sqrt{-g} \left[R + \frac{1}{2} g^{\mu\nu} \partial_\mu \phi \partial_\nu \phi + V(\phi) \right]. \quad (7)$$

The scalar field ϕ is a function of radial coordinate r alone. The self-interaction of the scalar field is taken in a form as in Eq. (4), i.e., $V(\phi) = V_0 + \frac{1}{2} M(\phi) \phi^2 + \frac{\lambda}{4} \phi^4$. We write a general static spherically symmetric metric tensor as

$$ds^2 = -G(r) dt^2 + G(r)^{-1} dr^2 + S(r)^2 d\Omega^2, \quad (8)$$

where the metric coefficients are also functions of r alone. The coordinates have natural domains, as in

$$r \in (-\infty, +\infty); \quad t \in (-\infty, +\infty); \quad \theta \in [0, \pi]; \quad \phi \in (-\pi, \pi]. \quad (9)$$

We proceed with an ansatz over the radius of two-sphere $S(r) = e^{-\sigma(r)}$. As we have already discussed in the introduction, V_0 will be treated as a parameter. $M(\phi)$ is expected to introduce a variation in the effective mass-like term for the scalar field ϕ and will be determined from the field equations of the theory. By varying the action with respect to the metric tensor and the scalar field ϕ , we find the following set of coupled differential equations for the functions $\sigma(r)$, $G(r)$, and $\phi(r)$,

$$\sigma'' - (\sigma')^2 + \frac{1}{4} (\phi')^2 = 0, \quad (10)$$

$$G'' - 2G'\sigma' - V(\phi) = 0, \quad (11)$$

$$G'' - 2G(2(\sigma')^2 - \sigma'') + 2e^{2\sigma} = 0. \quad (12)$$

We write an exact solution to these field equations as

$$\sigma(r) = -\frac{1}{2} \ln(r^2 + a^2), \quad (13)$$

$$G(r) = 1 + C_1 + \frac{C_2}{2a^3} [ar + (a^2 + r^2) \tan^{-1}(r/a)], \quad (14)$$

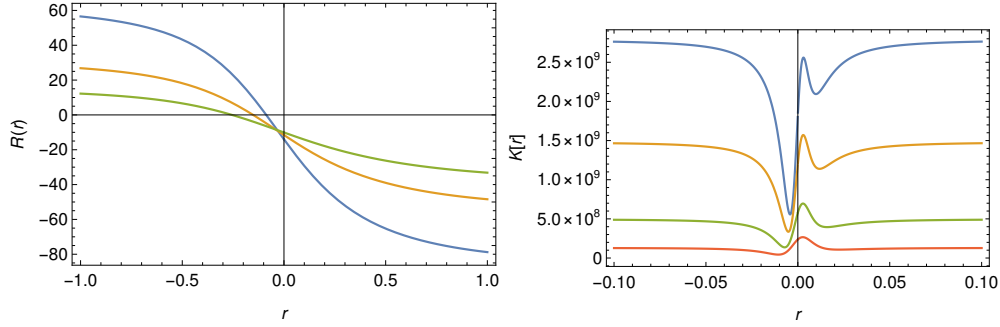


Figure 1: Ricci scalar $R(r)$ and Kretschmann scalar $K(r)$ as a function of r for different values of a . The parameter choices made in this graph are $C_1 = 1$ and $C_2 = 0.01$, while the parameter a is varied.

$$\phi(r) = C_3 \pm 2 \tan^{-1}(r/a). \quad (15)$$

a is a non-zero parameter of the solution. C_1 , C_2 and C_3 are constants of integration. The functional form of $\sigma(r)$ exhibits logarithmic behavior at large distances, suggesting that the radial function falls off slowly. There can be two different profiles for the scalar field depending on the \pm sign after the parameter C_3 . Due to the presence of $\tan^{-1}(r/a)$ in the profile, the scalar field always asymptotes to constant values at large r .

The first crucial property of this space-time metric is the regularity of curvature scalars. We calculate the Ricci and Kretschmann scalars as

$$R = -\frac{6a^7C_1 + 2a^5(9C_1r^2 + 1) + a^3(12C_1r^4 + 7C_2r) + 3C_2(a^4 + 3a^2r^2 + 2r^4)\tan^{-1}\left(\frac{r}{a}\right) + 6aC_2r^3}{a^3(a^2 + r^2)^2} \quad (16)$$

$$K = \left[3C_2^2(a^2 + r^2)^2(a^4 + 2a^2r^2 + 2r^4)\tan^{-1}\left(\frac{r}{a}\right)^2 + 2aC_2(a^2 + r^2)\tan^{-1}\left(\frac{r}{a}\right)(6a^8C_1 + 2a^6(9C_1r^2 + 2) + a^4r(24C_1r^3 + 5C_2 + 2r) + 2a^2(6C_1r^6 + 5C_2r^3) + 6C_2r^5) + a^2(12a^{12}C_1^2 + 16a^{10}C_1(3C_1r^2 + 1) + 4a^8(21C_1^2r^4 + C_1r(5C_2 + 6r) + 3) + 4a^6(C_2r(15C_1r^2 + 4) + 2C_1r^4(9C_1r^2 + 1)) + a^4r^2(24C_1^2r^6 + 4C_2(16C_1r^3 + r) + 11C_2^2) + 2a^2C_2r^4(12C_1r^3 + 7C_2) + 6C_2^2r^6) \right] \left[a^6(a^2 + r^2)^4 \right]^{-1}. \quad (17)$$

It is straightforward to note that the scalars do not diverge for any value of r . In particular, there is no singularity at $r = 0$ as long as a is treated as a non-zero parameter and throughout this article we keep the parameter that way. The role of this parameter resembles the recently proposed solution of a regular black hole [53] and its time-evolving analogue [54]. We plot the scalars as a function of radial coordinate in Fig. 1 to prove our claim. For the purpose of this plot, we have chosen $C_1 = 1$ and $C_2 = 0.01$, while the parameter a is being varied. Using the exact form of the metric coefficients, it is also straightforward to calculate the components of the energy-momentum tensor (using the mixed components of the field equations $G_\nu^\mu = 8\pi G_N T_\nu^\mu$). The density is given by $\rho = -T_t^t$ and the radial pressure is given by $p_r = T_r^r$. Furthermore, we can check if there is any violation of Null Energy Condition (NEC) inside the spherical

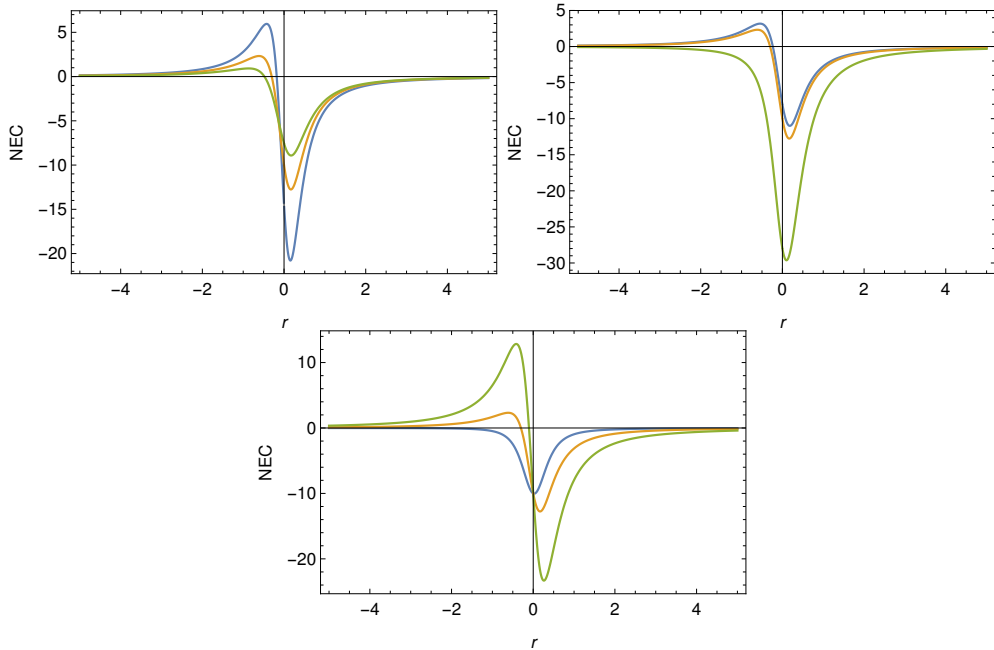


Figure 2: Null Energy Condition as a function of r for different values of a , C_1 and C_2 . Top left : $C_1 = C_2 = 1$ while a is being varied. Top right : $a = 0.5$ and $C_2 = 1$, C_1 is being varied from 0.01 to 1. Below : $a = 0.5$ and $C_1 = 1$ while C_2 is being varied from 0.1 to 10.

geometry. The necessary condition for an NEC to be valid is that the sum of density and radial pressure should be positive. Any violation of NEC is directly connected to the idea of a Null Convergence Condition (NCC), which is a characteristic of wormhole geometry, where radial null rays can defocus around the wormhole throat [55–59]. We plot the NEC profile in Fig. 2 as a function of r . For the graph on the top left of Fig. 2, we keep the two parameters C_1 and C_2 fixed at unity and vary the parameter a . For the graph on top right, we keep a fixed at 0.5 and C_2 fixed at 1 while varying C_1 from 0.01 to 1. For the graph below, we keep a fixed at 0.5 and C_1 fixed at 1 while varying C_2 from 0.1 to 10.

We plot the scalar field profile as a function of r in Fig. 3. The blue curve is the profile for a minus sign in $C_3 \pm 2 \tan^{-1}(r/a)$, while the orange curve is for the plus sign. The constant C_3 is taken to be unity. It is seen that for both of the choices, the scalar field behaves as a constant at a large r . Finally, the solution for $M(\phi)$ is written straightaway from the field equations as

$$M = 2 \left\{ G'' + \frac{2G'r}{(r^2 + a^2)} - V_0 - \frac{\lambda}{4} \phi^4 \right\}. \quad (18)$$

It is important to note that the solution we have found is consistent if and only if $M(\phi)$ is a function. If it is a constant, then the requirement that $[G'' + \frac{2G'r}{(r^2 + a^2)} - V_0 - \frac{\lambda}{4} \phi^4]$ introduces a steep constraint on the allowed solution spectrum. In Fig. 4 we plot $M(\phi)$ as a function of r for $\phi(r) = C_3 + 2 \tan^{-1}(r/a)$. The graph on the top left is for different values of a while the three other parameters C_1 , C_2 and C_3 are

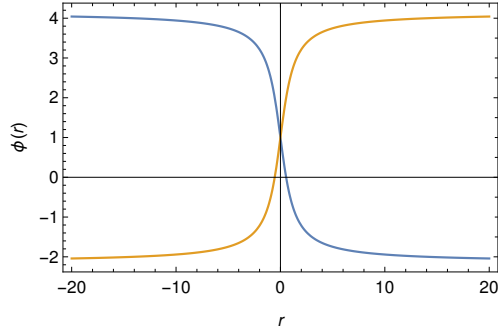


Figure 3: $\phi(r)$ as a function of r . The blue curve shows the profile for a minus sign in $C_3 \pm 2 \tan^{-1}(r/a)$, while the orange curve is for the plus sign. $C_3 = 1$.

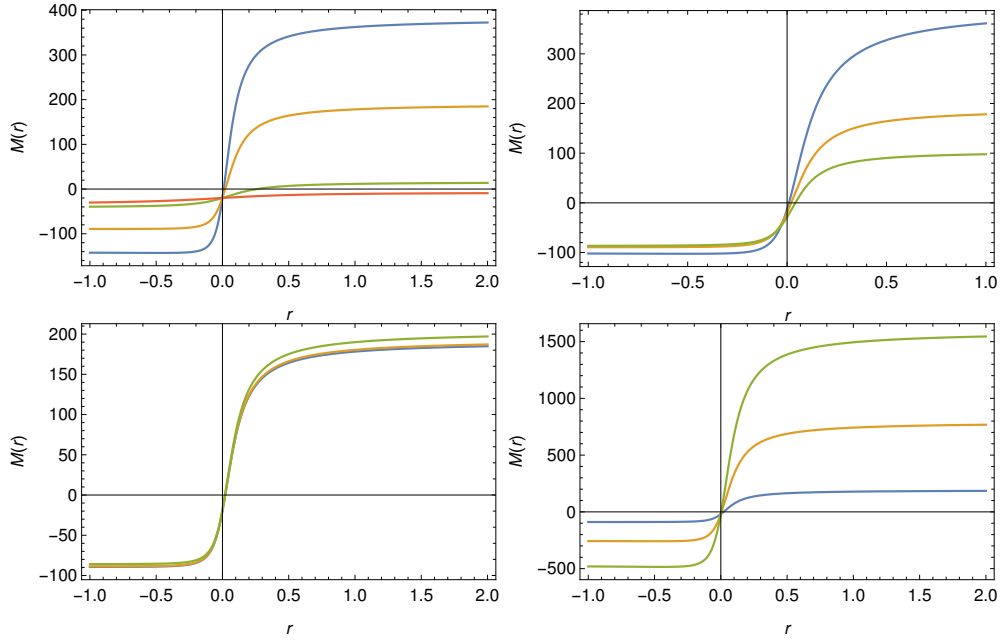


Figure 4: Plot of $M(\phi)$ as a function of r for $\phi(r) = C_3 + 2 \tan^{-1}(r/a)$. Top left : different values of a is considered while C_1 , C_2 and C_3 are fixed. Top right : different values of C_3 is considered while a , C_1 and C_2 are fixed. Bottom left : different values of C_1 is considered while a , C_2 and C_3 are fixed. Bottom right : different values of C_2 is considered while a , C_1 and C_3 are fixed.

fixed. The graph on top right is for different values of C_3 while a , C_1 and C_2 are fixed. The graph on bottom left is for different values of C_1 while a , C_2 and C_3 are fixed. The graph on bottom right is for different values of C_2 while a , C_1 and C_3 are fixed. Similarly, in Fig. 5 we plot $M(\phi)$ as a function of r for the second scalar field profile, $\phi(r) = C_3 - 2 \tan^{-1}(r/a)$. The graph on the top left is for different values

of a while the three other parameters C_1 , C_2 and C_3 are fixed. The graph on top right is for different values of C_3 while a , C_1 and C_2 are fixed. The graph on bottom left is for different values of C_1 while a , C_2 and C_3 are fixed. The graph on bottom right is for different values of C_2 while a , C_1 and C_3 are fixed. Irrespective of the choice of ϕ profile, the qualitative behavior of $M(\phi)$ remains the same as a function of r . There is always a switch from negative into positive values of $M(\phi)$ within a small neighbourhood of $r = 0$, but never exactly at $r = 0$. In a sense, the solution therefore behaves as in a *symmetron* where the interaction potential is taken as

$$V(\phi) = -\frac{1}{2}\mu^2\phi^2 + \frac{1}{4}\lambda\phi^4, \quad A(\phi) = 1 + \frac{1}{2M^2}\phi^2, \quad (19)$$

where $A(\phi)$ defines a universal coupling of the scalar field to the space-time metric in an Einstein frame [21, 60, 61]. The effective potential in this case becomes dependent on μ , M (two mass scales) and the constant λ , written as

$$V_{\text{eff}}(\phi) = \frac{1}{2} \left(\frac{\rho}{M^2} - \mu^2 \right) \phi^2 + \frac{1}{4} \lambda \phi^4. \quad (20)$$

Due to the negative mass term of $V(\phi)$ there is a spontaneous breakdown of \mathbf{Z}_2 symmetry. The sign of the quadratic term in the effective potential depends on the local matter density. As a result, the spontaneous breaking of \mathbf{Z}_2 symmetry is also dependent on the presence of the source. When $\rho = 0$, which corresponds to the region outside the source, the potential spontaneously breaks reflection symmetry, and the scalar field acquires a vacuum expectation value (VEV) $\phi_0 \equiv \mu/\sqrt{\lambda}$. However, within the source, if the parameters are chosen such that $\rho > M^2\mu^2$, the effective potential no longer induces symmetry breaking, and the VEV becomes zero. The present solution, however, also allows a few cases, where there is no transition from negative into positive, i.e., the spontaneous symmetry always remains broken throughout the coordinate range $r \in (-\infty, +\infty)$.

We now look into the radial null curves by setting the spacetime interval to zero. On a fixed plane ($d\theta = d\phi = 0$) such a curve can describe the path of a massless particle, such as a photon, moving radially through the spacetime, obeying

$$\frac{dr}{dt} = \pm \left[1 + C_1 + \frac{C_2}{2a^3} (ar + (a^2 + r^2) \tan^{-1}(r/a)) \right]. \quad (21)$$

One can define a coordinate speed of light in the spacetime metric as $c(r) = \left| \frac{dr}{dt} \right|$. The coordinate speed of light $c(r)$ depends on the radial coordinate r and is naturally affected by the curvature of spacetime. In flat, uncurved spacetime, the speed of light is supposed to be constant, but in curved spacetime, the speed of light should vary depending on the location within the gravitational field. An effective refractive index $n(r)$ can also be defined as the inverse of the coordinate speed of light, $n(r) = \frac{1}{c(r)}$. It describes how the curvature of spacetime affects the propagation of light. If $c(r)$ is reduced compared to the standard value of the speed of light, the refractive index $n(r)$ is increased, indicating that light effectively slows down as it passes through these regions. Effectively, the function $n(r)$ provides a measure of the gravitational lensing effects in the spacetime. Gravitational lensing occurs because light rays are bent and slowed down as they pass through regions of spacetime with strong curvature, which is analogous to the way light bends and slows down when passing through a medium with a varying refractive index in optics.

We use Eq. (21) to check if there is any formation of the horizon for any value or range of r , for which we simply require that $\frac{dr}{dt} = 0$ for any $r \in (-\infty, +\infty)$. Given the fact that Eq. (21) is not straightforward

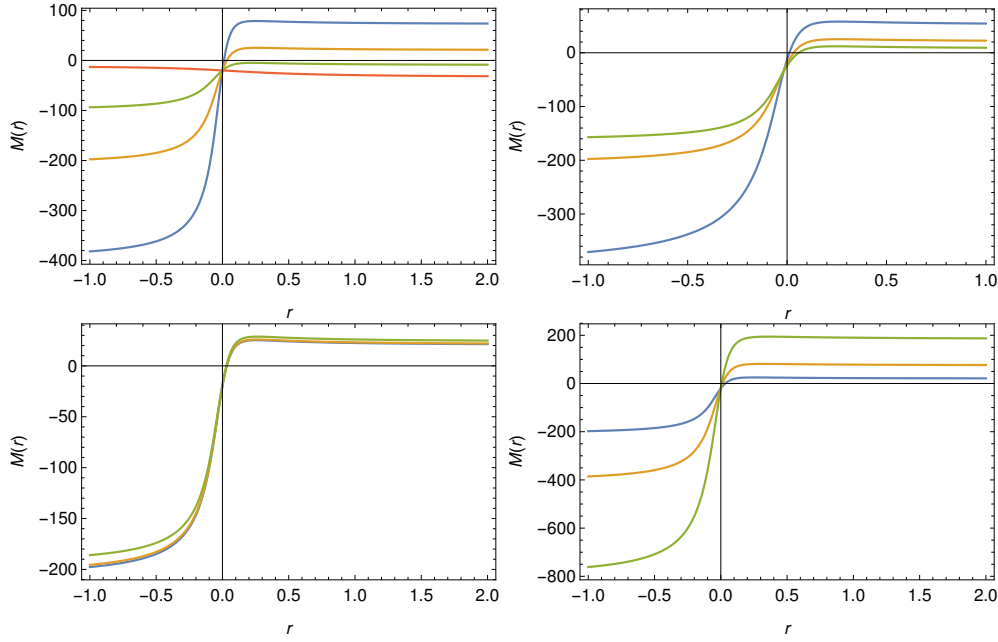


Figure 5: Plot of $M(\phi)$ as a function of r for $\phi(r) = C_3 - 2 \tan^{-1}(r/a)$. Top left : different values of a is considered while C_1 , C_2 and C_3 are fixed. Top right : different values of C_3 is considered while a , C_1 and C_2 are fixed. Bottom left : different values of C_1 is considered while a , C_2 and C_3 are fixed. Bottom right : different values of C_2 is considered while a , C_1 and C_3 are fixed.

to solve, primarily due to the presence of a \tan^{-1} term, we plot the RHS of the equation in Fig. 6. The graph on the top left is for a chosen set of $C_1 = 1$, $C_2 = 1$. We change the value of a and find that as long as $a \lesssim 0.9$, the curve intersects zero, and we can, in principle, have a horizon at some coordinate location. However, this is definitely not a black hole since we do not have any curvature singularities. It can be rendered as a one-way wormhole with an extremal null throat. However, for $a \gtrsim 0.9$, we have $\frac{dr}{dt} \neq 0$ for any $r \in (-\infty, +\infty)$ and therefore the metric represents a two-way traversable wormhole. For this set, $a \sim 0.9$ defines a threshold of horizon formation, however, this is not an exhaustive analysis. For a different set $C_1 = 1$, $C_2 = 3$ (graph on top right), the threshold value of a is found to be ~ 1.25 . The bottom left graph is for a fixed set of $a = C_2 = 1$, while the parameter C_1 is varied, and for this set, we do not have any formation of horizon. The bottom right graph is for a fixed set of $a = C_1 = 1$, while the parameter C_2 is varied.

In order to have a mathematical argument behind this parameter-dependence of horizon formation we approximate Eq. (21) around a very small neighbourhood of $r = 0$ (essentially to ignore any terms $\sim O(r^3)$) or higher. Under this approximation $\tan^{-1}(\frac{r}{a}) \approx \frac{r}{a}$, and the radial null geodesic curve equation becomes a quadratic equation

$$C_1 r_h^2 + \frac{C_2}{a^2} r_h + (1 + C_1 a^2) = 0. \quad (22)$$

Since we are expecting the coordinate location of a *horizon*, it is better to use r_h in place of r . By the

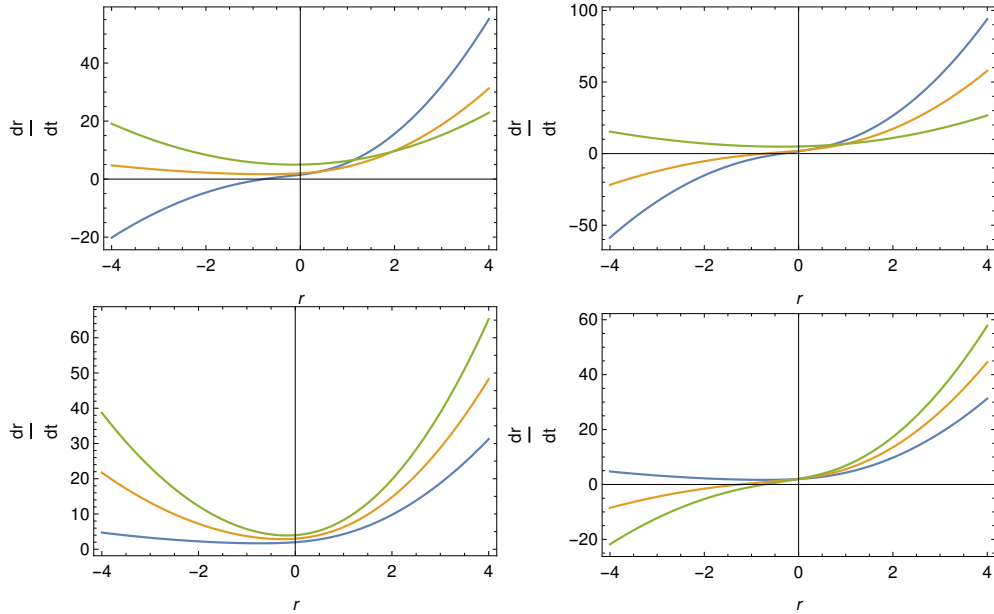


Figure 6: $\frac{dr}{dt}$ as a function of r for different set of initial conditions. Top left : $C_1 = 1, C_2 = 1$ and the value of a is varied. Top right : $C_1 = 1, C_2 = 3$ and the value of a is varied. Bottom left : $a = C_2 = 1$, while the parameter C_1 is varied. Bottom right : $a = C_1 = 1$, while the parameter C_2 is varied.

standard method of treating quadratic equations, this must have two roots defined as

$$r_h = -\frac{C_2}{a^2} \pm \frac{\sqrt{C_2^2 - 4a^4C_1(1 + C_1a^2)}}{2a^2C_1}. \quad (23)$$

Therefore we make a deduction that the realistic coordinate location of the horizon can only be found as long as $C_2^2 - 4a^4C_1(1 + C_1a^2) \geq 0$ or $C_2^2 \geq 4a^4C_1(1 + C_1a^2)$.

3 Photon sphere, Lyapunov exponent, Shadow radius, and Innermost Stable Circular Orbits

In this section, we discuss a few additional properties of this space-time metric: the radius of the photon sphere (r_{ph}), the shadow radius (r_{sh}), the innermost stable circular orbits (r_{ISCO}) and the Lyapunov exponent (λ). While a photon sphere is associated with massless particles, an ISCO is related to massive particles [62–66]. In particular, the existence of a photon circular orbit plays a crucial role in understanding the characteristic signatures of the quasi-normal modes and shadow radius. We parametrize the tangent vector to the worldline of any particle (massless or massive) by an affine parameter τ and write

$$g_{ab} \frac{dx^a}{d\tau} \frac{dx^b}{d\tau} = -g_{tt} \left(\frac{dt}{d\tau} \right)^2 + g_{rr} \left(\frac{dr}{d\tau} \right)^2 + (r^2 + a^2) \left\{ \left(\frac{d\theta}{d\tau} \right)^2 + \sin^2 \theta \left(\frac{d\phi}{d\tau} \right)^2 \right\}. \quad (24)$$

The cases we are interested in are timelike (massive particle) and null (massless particle) and are classified as

$$ds^2/d\lambda^2 = \epsilon \quad , \quad \epsilon = \begin{cases} -1 & \text{timelike worldline} \\ 0 & \text{null worldline.} \end{cases} \quad (25)$$

For a spherically symmetric metric once again we take $\theta = \frac{\pi}{2}$ and write equations on an equatorial plane as

$$g_{ab} \frac{dx^a}{d\lambda} \frac{dx^b}{d\lambda} = -g_{tt} \left(\frac{dt}{d\lambda} \right)^2 + g_{rr} \left(\frac{dr}{d\lambda} \right)^2 + (r^2 + a^2) \left(\frac{d\phi}{d\lambda} \right)^2 = \epsilon . \quad (26)$$

Using the Killing symmetries we can express $\frac{dt}{d\lambda}$ and $\frac{d\phi}{d\lambda}$ in terms of conserved energy E and angular momentum L per unit mass [67] as

$$G(r) \left(\frac{dt}{d\lambda} \right) = E ; \quad (r^2 + a^2) \left(\frac{d\phi}{d\lambda} \right) = L, \quad (27)$$

where, we recall that $G(r) = 1 + C_1 + \frac{C_2}{2a^3} [ar + (a^2 + r^2) \tan^{-1}(r/a)]$ for the exact solution considered here. Combining Eq. (26) and Eq. (27) we derive

$$\left(\frac{dr}{d\lambda} \right)^2 = E^2 + G(r) \left\{ \epsilon - \frac{L^2}{r^2 + a^2} \right\}, \quad (28)$$

from which we can write an effective potential for any geodesic orbit as follows

$$V_\epsilon(r) = G(r) \left\{ -\epsilon + \frac{L^2}{r^2 + a^2} \right\} . \quad (29)$$

For a massless particle $\epsilon = 0$. In a spherically symmetric environment, the r values which can generate $V'_0(r) = 0$ give the coordinate locations sufficiently close to the mass enclosed within the metric, so that photons are restricted to travel along circular geodesic orbits only. The effective potential for such a case is written as $V_0(r) = G(r) \left(\frac{\mathbb{L}^2}{r^2 + a^2} \right)$. The radius of the circular photon orbit, r_{ph} is calculated by setting $V'_0(r) = 0$ [68–71], leading to the condition

$$2rG = (a^2 + r^2)G' \Rightarrow \frac{L^2(C_2 - 2r_{\text{ph}})}{(a^2 + r_{\text{ph}}^2)^2} \Rightarrow r_{\text{ph}} = \frac{C_2}{2}. \quad (30)$$

A circular photon orbit is stable or unstable depending on the signature of V''_0 evaluated at r_{ph} . An explicit form can be calculated as

$$V''_0(r) \Big|_{r_{\text{ph}}} = -\frac{2L^2 \left\{ a^2 + \frac{C_2^2}{4} \right\}}{(a^2 + r_{\text{ph}}^2)^3}, \quad (31)$$

which is always negative and confirms the existence of unstable photon orbits in this spacetime. This behavior is independent of the choice of a . This is demonstrated in Fig. 7 and Fig. 8 by plotting the effective potential and its' second derivative as a function of a , taking $\mathbb{L} = 2$.

The Lyapunov exponent is determined by studying small perturbations around the radial null trajectory. We examine how the effective potential, V_0 , varies with a small perturbation δr as the radial coordinate approaches the photon orbit at $r = r_{\text{ph}}$. This leads us to an expression for the evolution of

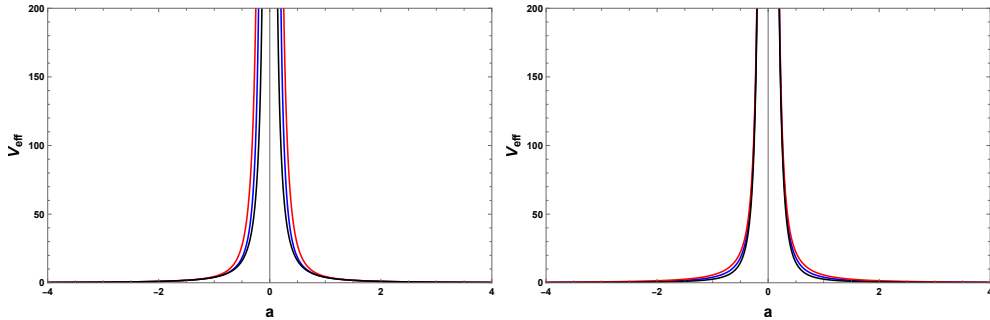


Figure 7: Left: Change of effective potential at the photon sphere with a for two sets: Left $\rightarrow C_1 = 1$ and different values of C_2 changing. Right $\rightarrow C_2 = 1$ and different values of C_1 . In both graphs, the angular momentum parameter is set to $L = 2$.

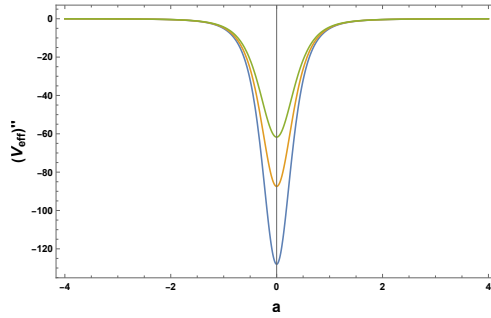


Figure 8: Second derivative of the effective potential at the photon sphere for different values of a and varying C_2 , with the angular momentum parameter fixed at $L = 2$.

the perturbation, given by $\delta r \sim \exp(\lambda t)$, where λ is the Lyapunov exponent. The Lyapunov exponent quantifies the rate at which these perturbations grow or decay over time, characterizing the stability of the orbit. It can be expressed in terms of the metric coefficient using the formula [72–75]

$$\lambda = \sqrt{\frac{G(r_{\text{ph}})}{2} \left(\frac{2G(r_{\text{ph}})}{r_{\text{ph}}^2} - G''(r_{\text{ph}}) \right)}. \quad (32)$$

This defines a direct correlation between the dynamics of the trajectory and the underlying spacetime geometry. Using the exact solution for $G(r)$ and the radius of the photon sphere, we calculate the Lyapunov exponent as

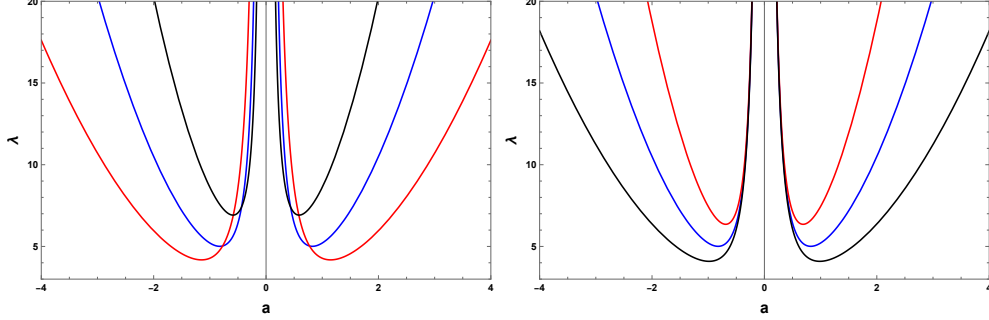


Figure 9: Left: Plot of the Lyapunov exponent as a function of a , for $C_1 = 1$ and different values of C_2 . Right: Plot of the Lyapunov exponent as a function of a , for $C_2 = 1$ and different values of C_1 .

$$\lambda = \frac{1}{2} \sqrt{\frac{\left(2(a^3 C_1 + a) + C_2 \cot^{-1}\left(\frac{2a}{C_2}\right)\right) \left(8a^5 C_1 + 2a^3 (C_1 C_2^2 + 4) + (4a^2 C_2 + C_2^3) \cot^{-1}\left(\frac{2a}{C_2}\right) + 4a C_2^2\right)}{a^4 C_2^2}}. \quad (33)$$

We plot λ in Fig. 9 as a function of a . A positive Lyapunov exponent signifies that nearby trajectories diverge over time, indicating a strong sensitivity to initial conditions.

The "shadow radius" of a compact object refers to the apparent size of the dark shape cast by the compact object against the backdrop of light, usually from a bright source behind it. A critical impact parameter can be defined as one that corresponds to the boundary between light rays that escape to infinity and those that are captured by the geometry (which in this case is either a one-way or a traversable wormhole). The shadow radius r_{sh} can be calculated by finding the critical parameter associated with null geodesics [76] using the equation

$$\frac{1}{r_{sh}^2} = \frac{G(r_{ph})}{(r_{ph}^2 + a^2)} \Rightarrow r_{sh} = \sqrt{\frac{2a^3}{2a^3 C_1 + C_2 \tan^{-1}\left(\frac{C_2}{2a}\right) + 2a}}. \quad (34)$$

In Fig. 10, we plot the shadow radius as a function of a for different sets of C_1 and C_2 .

In order to study the geodesic orbit for massive particles, we consider timelike worldline, i.e., $\epsilon = -1$ in Eq. (29). The innermost stable circular orbit primarily corresponds to the condition that the effective potential experienced by the particle must obey $V'_{-1} = 0$ [75]. This condition can be simplified into

$$2a^7 C_1 r + a C_2 r^4 + a^5 (C_2 + 4C_1 r^3) + a^3 (C_2 L^2 - 2L^2 r + 2C_2 r^2 + 2C_1 r^5) + C_2 r (a^2 + r^2) \tan^{-1}\left(\frac{r}{a}\right) = 0. \quad (35)$$

One can solve this equation numerically, however it is better to proceed with a fixed coordinate value $r = r_c$ where a circular orbit is expected to form. Thereafter, it is possible to derive a required angular momentum, L_c , in terms of r_c , a , C_1 , and C_2 . In this context, the innermost circular orbit for a massive particle will simply be the coordinate value of r_c , which can minimize L_c . Since with a $\tan^{-1}\left(\frac{r_c}{a}\right)$ term,

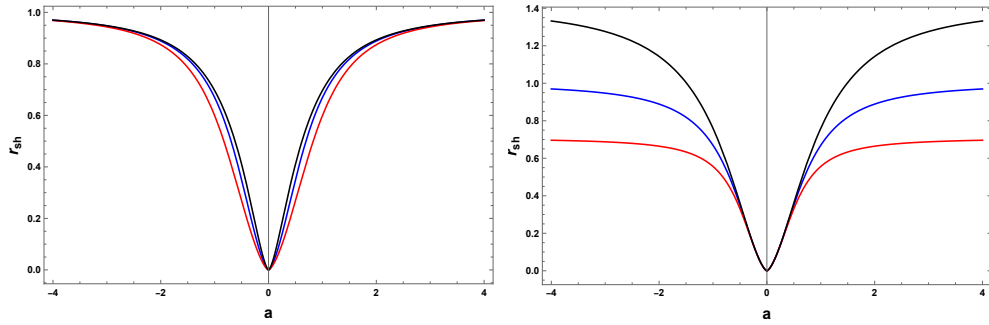


Figure 10: Left: Shadow radius as a function of a for $C_1 = 1$ and different values of C_2 . Right: Shadow radius as a function of a for $C_2 = 1$ and different values of C_1 .

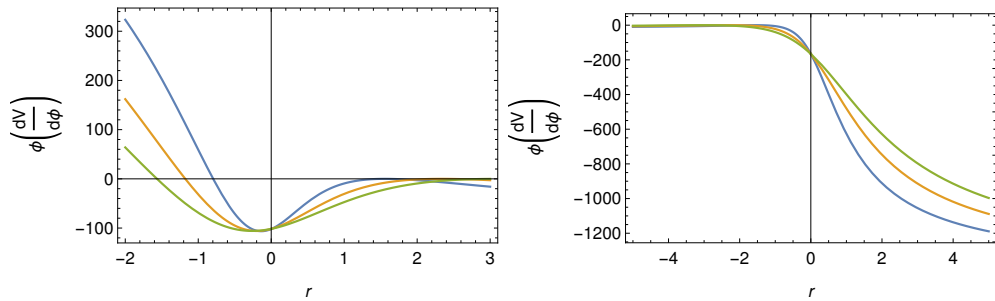


Figure 11: $\phi \frac{dV}{d\phi}$ as a function of r for two different profiles of scalar field $\phi(r) = C_3 \pm 2 \tan^{-1}(r/a)$.

it is non-trivial to proceed, once again, we study the condition within a small neighborhood around $r = 0$. Within this limit we approximate $\tan^{-1}\left(\frac{r}{a}\right) \simeq \frac{r}{a}$ and neglect the higher order terms of r_c to ultimately find

$$L_c = \sqrt{\frac{2a^7 C_1 r_c + a^5 C_2}{a^3 (C_2 - 2r_c)}}. \quad (36)$$

We can compare this expression with circular orbits in weak-field GR. In classical physics, the angular momentum per unit mass for a particle with angular velocity ω is $L_c \sim \omega r_c$. Kepler's third law of planetary motion implies that $\omega^2 \sim \frac{G_N m}{r_c}$, where m is the mass of a central object. Therefore we can write that

$$L_c \sim \sqrt{\frac{G_N m}{r_c}} r_c \Rightarrow L_c \sim \sqrt{m r_c}. \quad (37)$$

Since our solution has no Schwarzschild limit, there is no direct mass parameter involved in this metric. However, compared with the weak field limit, we note that the parametric combination of $\frac{2a^4 C_1}{C_2}$ might have a correlation with a corresponding mass function.

We conclude with a remark and reminder that the condition $\phi \frac{dV}{d\phi} \geq 0$ is usually treated as a requirement such that the self-interaction potential has a local minimum at $\phi = 0$ and no local maximum within the ϕ -range considered. This condition serves as the key to effectively rule out non-trivial scalar deformations of the Schwarzschild solution. For the present solution it can be seen in Fig. 11 that the condition is always violated irrespective of the scalar field profile under consideration.

4 Conclusion

The exact solution presented in this article represents a system of static spherically symmetric general relativity plus a massive scalar field. The scalar self interaction is Higgs type as in a linear combination of quadratic and quartic terms. It is found that for the solution to be consistent the coefficient of the quadratic term, as in the mass term M , must be a function of coordinates (in the form of Eq. Eq. (4)). This enforces a spontaneous symmetry breaking in the system. The solution does not exhibit any singularity as checked from the curvature scalar profiles which remain finite for all possible coordinate ranges. The behavior of radial null geodesics demonstrates that the metric represents either a one-way wormhole or a two-way traversable wormhole, depending on the parameter space. We compute and discuss properties of the photon sphere, Lyapunov exponent, shadow radius and the radius of the innermost stable circular orbits that can be accommodated by this spacetime metric. It may be an interesting prospect to compare this solution with *dirty* black holes [77–79], associated with non-trivial stress-energy tensor or even with regular black holes [53]. This is usually done through an analysis of the derived metric tensor in a generalized tortoise coordinate and subsequent derivation of Regge-Wheeler equations for spin zero, spin one and/or spin two particles coupled to gravity. This shall be discussed in a follow-up article. The metric solution is novel as it does not reduce to the Schwarzschild metric in any limit. Moreover, it opens up an intriguing thought: to associate spontaneous symmetry breaking with a threshold of wormhole throat formation.

Acknowledgement

Soumya Chakrabarti acknowledges the IUCAA for providing facility and support under the visiting associateship program. Acknowledgment is also given to Vellore Institute of Technology for the financial support through its Seed Grant (No. SG20230027), the year 2023.

References

- [1] K. Schwarzschild, *Sitzungsber. Preuss. Akad. Wiss. Phys. Math. Kl.*, , physics/9905030 (1916), [arXiv:physics/9905030 \[physics.hist-ph\]](#) .
- [2] D. Hilbert, *Nachr. Ges. Wiss. Math. Phys. Kl. (Göttingen)* , 53 (1917).
- [3] H. Weyl, *Ann. d. Phys.* **54**, 117 (1917).
- [4] J. T. Jebsen, *Ark. Mat. Ast. Fys. (Stockholm)* **15**, 18 (1921).
- [5] G. D. Birkhoff, *Relativity and Modern Physics*, Harvard University Press **253**, 18 (1923).
- [6] K. Sato, *Journal of Astrophysics and Astronomy Supplement* **16**, 37 (1995).

- [7] O. Bechmann and O. Lechtenfeld, *Class. Quant. Grav.* **12**, 1473 (1995), [arXiv:gr-qc/9502011](#) .
- [8] J. D. Bekenstein, in *2nd International Sakharov Conference on Physics* (1996) pp. 216–219, [arXiv:gr-qc/9605059](#) .
- [9] C. A. R. Herdeiro and E. Radu, *International Journal of Modern Physics D* **24**, 1542014 (2015).
- [10] C. Barceló, R. Carballo-Rubio, and S. Liberati, *Classical and Quantum Gravity* **36**, 13LT01 (2019).
- [11] S. Perlmutter *et al.* (Supernova Cosmology Project), *Bull. Am. Astron. Soc.* **29**, 1351 (1997), [arXiv:astro-ph/9812473](#) .
- [12] A. G. Riess, A. V. Filippenko, P. Challis, A. Clocchiatti, A. Diercks, P. M. Garnavich, R. L. Gilliland, C. J. Hogan, S. Jha, R. P. Kirshner, B. Leibundgut, M. M. Phillips, D. Reiss, B. P. Schmidt, R. A. Schommer, R. C. Smith, J. Spyromilio, C. Stubbs, N. B. Suntzeff, and J. Tonry, *The Astronomical Journal* **116**, 1009 (1998).
- [13] A. Melchiorri, P. A. R. Ade, P. de Bernardis, J. J. Bock, J. Borrill, A. Boscaleri, B. P. Crill, G. D. Troia, P. Farese, P. G. Ferreira, K. Ganga, G. de Gasperis, M. Giacometti, V. V. Hristov, A. H. Jaffe, A. E. Lange, S. Masi, P. D. Mauskopf, L. Miglio, C. B. Netterfield, E. Pascale, F. Piacentini, G. Romeo, J. E. Ruhl, and N. Vittorio, *The Astrophysical Journal* **536**, L63 (2000).
- [14] A. E. Lange, P. A. R. Ade, J. J. Bock, J. R. Bond, J. Borrill, A. Boscaleri, K. Coble, B. P. Crill, P. de Bernardis, P. Farese, P. Ferreira, K. Ganga, M. Giacometti, E. Hivon, V. V. Hristov, A. Iacoangeli, A. H. Jaffe, L. Martinis, S. Masi, P. D. Mauskopf, A. Melchiorri, T. Montroy, C. B. Netterfield, E. Pascale, F. Piacentini, D. Pogosyan, S. Prunet, S. Rao, G. Romeo, J. E. Ruhl, F. Scaramuzzi, and D. Sforza, *Phys. Rev. D* **63**, 042001 (2001).
- [15] T. Padmanabhan and T. R. Choudhury, *Monthly Notices of the Royal Astronomical Society* **344**, 823 (2003), <https://academic.oup.com/mnras/article-pdf/344/3/823/3304941/344-3-823.pdf> .
- [16] I. Zlatev, L. Wang, and P. J. Steinhardt, *Phys. Rev. Lett.* **82**, 896 (1999).
- [17] V. Sahni and A. Starobinsky, *International Journal of Modern Physics D* **09**, 373 (2000).
- [18] E. G. Adelberger, B. R. Heckel, and A. E. Nelson, *Ann. Rev. Nucl. Part. Sci.* **53**, 77 (2003), [arXiv:hep-ph/0307284](#) .
- [19] J. A. Frieman, C. T. Hill, A. Stebbins, and I. Waga, *Phys. Rev. Lett.* **75**, 2077 (1995).
- [20] J. Khoury and A. Weltman, *Phys. Rev. Lett.* **93**, 171104 (2004).
- [21] K. Hinterbichler and J. Khoury, *Phys. Rev. Lett.* **104**, 231301 (2010).
- [22] S. Chakrabarti, K. Dutta, and J. L. Said, *Monthly Notices of the Royal Astronomical Society* **514**, 427 (2022), <https://academic.oup.com/mnras/article-pdf/514/1/427/43946981/stac1321.pdf> .
- [23] P. A. M. Dirac, *Nature* **139**, 323 (1937).
- [24] P. Jordan, *Naturwissenschaften* **25**, 513 (1937).
- [25] M. Fierz, *Helvetica Physica Acta* **29**, 128 (1956).

- [26] C. Brans and R. H. Dicke, *Phys. Rev.* **124**, 925 (1961).
- [27] G. Gamow, *Phys. Rev. Lett.* **19**, 759 (1967).
- [28] J. D. Bekenstein, *Phys. Rev. D* **25**, 1527 (1982).
- [29] J.-P. Uzan, *Rev. Mod. Phys.* **75**, 403 (2003).
- [30] T. Chiba, *Progress of Theoretical Physics* **126**, 993 (2011), [arXiv:1111.0092 \[gr-qc\]](#) .
- [31] J. Gasser and H. Leutwyler, *Physics Reports* **87**, 77 (1982).
- [32] X. Ji, *Phys. Rev. Lett.* **74**, 1071 (1995).
- [33] X. Calmet and H. Fritzsch, *Phys. Lett. B* **540**, 173 (2002), [arXiv:hep-ph/0204258](#) .
- [34] H. Fritzsch, *Nuclear Physics B - Proceedings Supplements* **186**, 221 (2009), proceedings of the QCD 08, 14th High-Energy Physics International Conference On Quantum ChromoDynamics.
- [35] J. Bagdonaite, E. J. Salumbides, S. P. Preval, M. A. Barstow, J. D. Barrow, M. T. Murphy, and W. Ubachs, *Phys. Rev. Lett.* **113**, 123002 (2014).
- [36] N. Huntemann, B. Lipphardt, C. Tamm, V. Gerginov, S. Weyers, and E. Peik, *Phys. Rev. Lett.* **113**, 210802 (2014).
- [37] J. Sola, E. Karimkhani, and A. Khodam-Mohammadi, *Class. Quant. Grav.* **34**, 025006 (2017), [arXiv:1609.00350 \[gr-qc\]](#) .
- [38] S. Chakrabarti, *Monthly Notices of the Royal Astronomical Society* **506**, 2518 (2021), <https://academic.oup.com/mnras/article-pdf/506/2/2518/39136152/stab1910.pdf> .
- [39] E. Battista, S. Capozziello, and A. Errehymy, (2024), [arXiv:2409.09750 \[gr-qc\]](#) .
- [40] E. Di Grezia, E. Battista, M. Manfredonia, and G. Miele, *Eur. Phys. J. Plus* **132**, 537 (2017), [arXiv:1707.01508 \[gr-qc\]](#) .
- [41] V. De Falco, E. Battista, S. Capozziello, and M. De Laurentis, *Phys. Rev. D* **101**, 104037 (2020), [arXiv:2004.14849 \[gr-qc\]](#) .
- [42] V. De Falco, E. Battista, S. Capozziello, and M. De Laurentis, *Phys. Rev. D* **103**, 044007 (2021), [arXiv:2101.04960 \[gr-qc\]](#) .
- [43] V. De Falco, E. Battista, S. Capozziello, and M. De Laurentis, *Eur. Phys. J. C* **81**, 157 (2021), [arXiv:2102.01123 \[gr-qc\]](#) .
- [44] X. Y. Chew and D.-h. Yeom, *Phys. Rev. D* **110**, 044036 (2024), [arXiv:2401.09039 \[gr-qc\]](#) .
- [45] X. Y. Chew, D.-h. Yeom, and J. L. Blázquez-Salcedo, *Phys. Rev. D* **108**, 044020 (2023), [arXiv:2210.01313 \[gr-qc\]](#) .
- [46] X. Y. Chew and K.-G. Lim, *Phys. Rev. D* **109**, 064039 (2024), [arXiv:2307.13972 \[gr-qc\]](#) .
- [47] X. Y. Chew and K.-G. Lim, *Universe* **10**, 212 (2024), [arXiv:2405.06407 \[gr-qc\]](#) .

- [48] X. Y. Chew and Y. S. Myung, *Phys. Rev. D* **110**, 044011 (2024), [arXiv:2405.04921 \[gr-qc\]](#) .
- [49] V. Dzhunushaliev, V. Folomeev, R. Myrzakulov, and D. Singleton, *JHEP* **07**, 094 (2008), [arXiv:0805.3211 \[gr-qc\]](#) .
- [50] C. F. S. Pereira, D. C. Rodrigues, J. C. Fabris, and M. E. Rodrigues, *Phys. Rev. D* **109**, 044011 (2024).
- [51] C. F. S. Pereira, E. L. Martins, D. C. Rodrigues, J. C. Fabris, and M. E. Rodrigues, (2024), [arXiv:2405.07455 \[gr-qc\]](#) .
- [52] C. F. S. Pereira, D. C. Rodrigues, M. V. d. S. Silva, J. C. Fabris, M. E. Rodrigues, and H. Belich, (2024), [arXiv:2409.09182 \[gr-qc\]](#) .
- [53] A. Simpson and M. Visser, *Journal of Cosmology and Astroparticle Physics* **2019**, 042 (2019).
- [54] S. Chakrabarti and S. Kar, *Phys. Rev. D* **104**, 024071 (2021).
- [55] M. Visser, *Lorentzian wormholes: From Einstein to Hawking* (1995).
- [56] A. Einstein and N. Rosen, *Phys. Rev.* **48**, 73 (1935).
- [57] C. W. Misner and J. A. Wheeler, *Annals of Physics* **2**, 525 (1957).
- [58] C. A. Kolassis, N. O. Santos, and D. Tsoubelis, *Classical and Quantum Gravity* **5**, 1329 (1988).
- [59] H. G. Ellis, *Journal of Mathematical Physics* **14**, 104 (1973), https://pubs.aip.org/aip/jmp/article-pdf/14/1/104/19133700/104.1_online.pdf .
- [60] P. Brax, C. van de Bruck, D. F. Mota, N. J. Nunes, and H. A. Winther, *Phys. Rev. D* **82**, 083503 (2010).
- [61] K. Hinterbichler, J. Khoury, A. Levy, and A. Matas, *Phys. Rev. D* **84**, 103521 (2011).
- [62] K. S. Virbhadra and G. F. R. Ellis, *Phys. Rev. D* **62**, 084003 (2000), [arXiv:astro-ph/9904193](#) .
- [63] K. S. Virbhadra and G. F. R. Ellis, *Phys. Rev. D* **65**, 103004 (2002).
- [64] K. S. Virbhadra and C. R. Keeton, *Phys. Rev. D* **77**, 124014 (2008).
- [65] C.-M. Claudel, K. S. Virbhadra, and G. F. R. Ellis, *Journal of Mathematical Physics* **42**, 818 (2001), https://pubs.aip.org/aip/jmp/article-pdf/42/2/818/19220437/818.1_online.pdf .
- [66] K. S. Virbhadra, *Phys. Rev. D* **79**, 083004 (2009).
- [67] R. M. Wald, *General Relativity* (Chicago Univ. Pr., Chicago, USA, 1984).
- [68] S. Chakraborty, *Galaxies* **9**, 96 (2021), [arXiv:2111.04912 \[gr-qc\]](#) .
- [69] A. K. Mishra, S. Chakraborty, and S. Sarkar, *Phys. Rev. D* **99**, 104080 (2019), [arXiv:1903.06376 \[gr-qc\]](#) .
- [70] T. Berry, A. Simpson, and M. Visser, *Universe* **7**, 2 (2020), [arXiv:2008.13308 \[gr-qc\]](#) .

- [71] Z.-Y. Tang, Y. C. Ong, and B. Wang, *Class. Quant. Grav.* **34**, 245006 (2017), [arXiv:1705.09633 \[gr-qc\]](#) .
- [72] A. K. Mishra and S. Chakraborty, *Phys. Rev. D* **101**, 064041 (2020), [arXiv:1911.09855 \[gr-qc\]](#) .
- [73] M. Rahman, S. Chakraborty, S. SenGupta, and A. A. Sen, *JHEP* **03**, 178 (2019), [arXiv:1811.08538 \[gr-qc\]](#) .
- [74] V. Cardoso, J. a. L. Costa, K. Destounis, P. Hintz, and A. Jansen, *Phys. Rev. Lett.* **120**, 031103 (2018), [arXiv:1711.10502 \[gr-qc\]](#) .
- [75] V. Cardoso, A. S. Miranda, E. Berti, H. Witek, and V. T. Zanchin, *Phys. Rev. D* **79**, 064016 (2009), [arXiv:0812.1806 \[hep-th\]](#) .
- [76] S. Chandrasekhar, *The Mathematical Theory of Black Holes*, The International Series of Monographs on Physics (Oxford University Press, 1983).
- [77] M. Visser, *Phys. Rev. D* **46**, 2445 (1992).
- [78] M. Visser, *Phys. Rev. D* **48**, 583 (1993).
- [79] P. Boonserm, T. Ngampitipan, and M. Visser, *Phys. Rev. D* **88**, 041502 (2013).